*Tetrahedron* Vol. 49, No. 41, pp. 9235-9250, 1993
Printed in Great Britain

0040-4020/93 $6.00+.00


# BILIRUBIN CONFORMATION AND INTRAMOLECULAR STERIC BUTTRESSING. C(10)-*gem*-DIMETHYL EFFECT

**Meiqiang Xie, Darren L. Holmes and David A. Lightner***

Department of Chemistry, University of Nevada
Reno, Nevada 89557-0020 USA

(*Received in USA* 17 *February* 1993; *accepted* 16 *March* 1993)

***Abstract.*** Bilirubin prefers to adopt either of two enantiomeric, intramolecularly hydrogen bonded conformations shaped like ridge tiles. Such conformations may be deformed or destabilized through the action of non-bonded steric repulsions, such as from *gem*-dimethyl substitution at the central methylene group connecting the two central pyrrole rings, as in 10,10-dimethylglaucorubin (1), (2,10,10,18-tetramethylmesobilirubin-XIIIα). In the folded intramolecularly hydrogen bonded pigment conformation, such substitution forces the *gem*-dimethyls into close proximity to the $CH_2$ groups at the β position of the propionic acid chains, as detected by $^1$H-NMR NOE. It lowers the activation barrier to conformational enantiomerism, which proceeds at twice the rate of its parent (2) without the *gem*-dimethyls. Conformational energy maps of 1 and 2 from molecular dynamics calculations show stable isoenergetic local minima for 1 lying only 7 kcal/mole above the isoenergetic global minima; whereas, the local minima in 2 lie ~9 kcal/mole above the global minima.

## INTRODUCTION

Bilirubin-IXα, the cytotoxic yellow-orange pigment of jaundice,[1] is formed from heme in mammalian metabolism.[2] Although the structure of bilirubin is typically represented in extended form (Fig. 1A), the pigment is conformationally mobile like a two-blade propeller. The most important conformational changes follow from rotations about the C(9)-C(10) and C(10)-C(11) carbon-carbon single bonds, *viz.* rotation angles $\phi_1$ and $\phi_2$ respectively. Rotations of the pyrrole β-substituents are much less important, except for carbon-carbon single bond rotations in the propionic acid chains at C(8) and C(12), as will become evident. Rotations about the C(5)-C(6) and C(14)-C(15) carbon-carbon single bonds are relatively less important, and rotations about the C(4) and C(15) carbon-carbon double bonds are high energy processes, that are relatively inaccessible, except through photoexcitation.[1,3]

Rotations about $\phi_1$ and $\phi_2$ are significant because the dipyrrinone propeller blades are thereby forced to sweep out large spatial volumes, and the pigment can be transformed into a large number of very different shapes, which range from porphyrin-like ($\phi_1 \simeq \phi_2 \simeq 0°$) (Fig. 1B) to extended ($\phi_1 \simeq \phi_2 \simeq 180°$)

Dedicated to Professor Carl Djerassi on the occasion of his 70th birthday.

(Fig. 1A). These two planar or near-planar conformations have been shown in molecular dynamics calculations[3,4] to be among the highest energy. They are thus improbable and potentially misleading representations. The most stable conformation, as revealed by molecular dynamics calculations,[3,4] is one where the pigment adopts a folded shape (through rotations about $\phi_1$ and $\phi_2$) so as to minimize non-bonded steric repulsions. One folded conformation is considerably stabilized by intramolecular hydrogen bonding (Fig. 1C). Such hydrogen-bonded conformers have been found in crystals[5] and in solutions of bilirubin.[6]

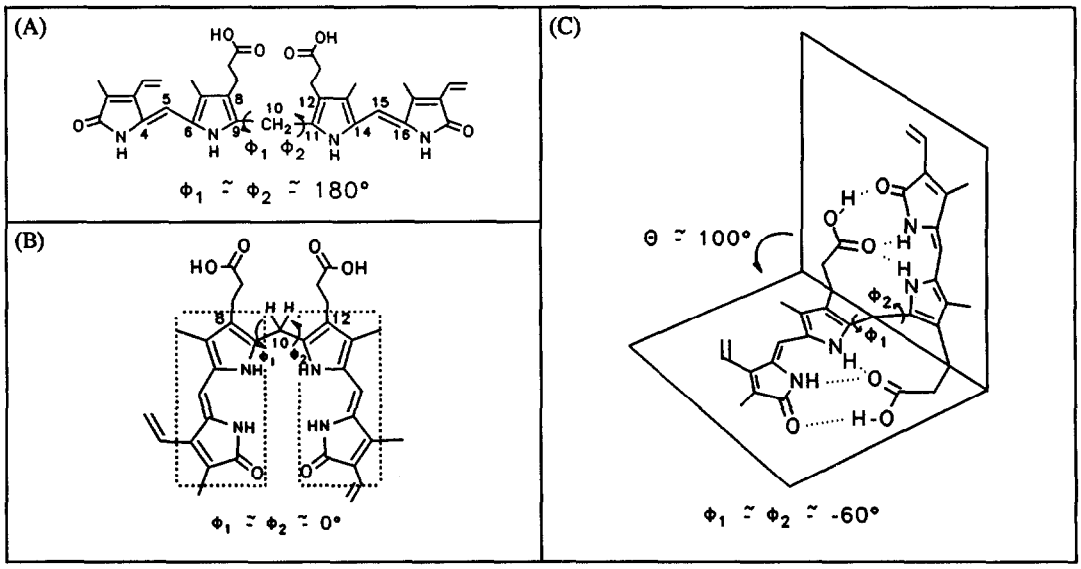


**FIGURE 1.** (A) Extended representation for bilirubin-IX$\alpha$, showing rotation angles, $\phi_1$ and $\phi_2$, about the C(9)-C(10) and C(10)-C(11) carbon-carbon single bonds, respectively. (B) Porphyrin-like representation, $\phi_1 \simeq \phi_2 \simeq 0°$, with dipyrrinone chromophores enclosed in dashed boxes. (C) Folded, intramolecularly hydrogen bonded conformation, $\phi_1 \simeq \phi_2 \simeq -60°$, shaped like a ridge-tile and corresponding to a global energy minimum conformation. The interplanar dihedral angle $\theta \simeq 100°$.

Bilirubin is a more elaborate analog of the simpler molecular propeller, diphenylmethane.[7] It has three elements that together have a dominating effect on its stereochemistry: (i) two dipyrrinone chromophores, each in a *syn*-periplanar conformation with *Z*-configuration C=C bonds (at C(4) or C(15)); (ii) an $sp^3$ carbon, C(10), which constrains the molecule to bend in the middle and allows the two dipyrrinone chromophores to rotate independently like propeller blades about $\phi_1$ and $\phi_2$; and (iii) two propionic acid groups, at C(8) and C(12), which can form intramolecular hydrogen bonds with the opposing dipyrrinone pyrrole and lactam functions. The strong preference for intramolecularly hydrogen-bonded conformers (Fig. 1C) in which polar groups are neutralized internally explains why bilirubin exhibits lipophilic behavior and requires covalent attachment of (polar) glucuronic acid for excretion.[2] It also explains why analogs with vinyl groups reduced to ethyl, *e.g.*, mesobilirubin-IX$\alpha$, or with methyl groups at all pyrrole $\beta$-positions, except C(8) and C(12), *e.g.*, glaucorubin (2),[8] exhibit similar solubility properties: soluble in $CHCl_3$, insoluble in $CH_3OH$, insoluble in dilute aqueous bicarbonate. In contrast, isomers that do not have their propionic acid groups located at C(8) and C(12), *e.g.*, mesobilirubin-IV$\alpha$, are known to have very different solubility properties: insoluble in chloroform, soluble in methanol and soluble in dilute aqueous bicarbonate.[9]

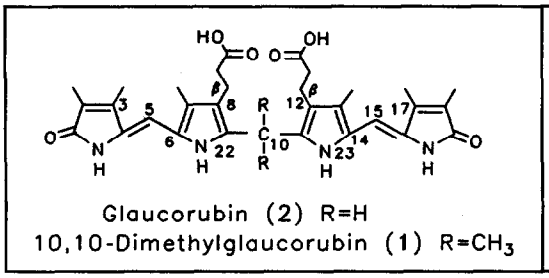


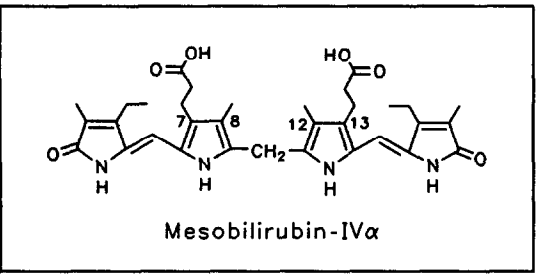


There are, however, more subtle non-bonded steric interactions that might be expected to perturb intramolecular hydrogen bonding and alter the properties of the pigment through allosteric action, *e.g.*, the *gem*-dimethyl effect of 10,10-dimethylglaucorubin (**1**). In the following, we describe the conformational analysis of **1** and **2** by NMR, and molecular dynamics. These results are correlated with an analysis of conformation by circular dichroism of optically active derivatives (*S*-alanine methyl ester bis-amides), and an investigation of the optical activity of **1** and **2** induced by quinine and by human serum albumin.

## RESULTS AND DISCUSSION

***Conformation from Molecular Dynamics.*** Like bilirubin (Fig. 1), glaucorubin (**2**) and its 10,10-dimethyl analog (**1**) may be viewed as two-blade molecular propellers, where the blades consist of dipyrrinones connected to a $-CH_2-$ or $-C(CH_3)_2-$ at C(10). As such, they are related to the simpler propellers, diphenylmethane and 2,2-diphenylpropane, studied and analyzed by Mislow *et al.*[7] Force-field analyses suggest that the former prefers the $C_{2v}$ gable conformation over the $C_2$ propeller geometry, but the latter prefers the $C_2$ or propeller conformation by ~3 kcal/mole (Fig. 2). A *gem*-dimethyl apparently has a moderate stabilizing effect on the $C_2$ conformation. So a *gem*-dimethyl group might also be expected to stabilize the $C_2$ conformation in other molecular propellers, such as 10,10-dimethyl analogs of bilirubin.

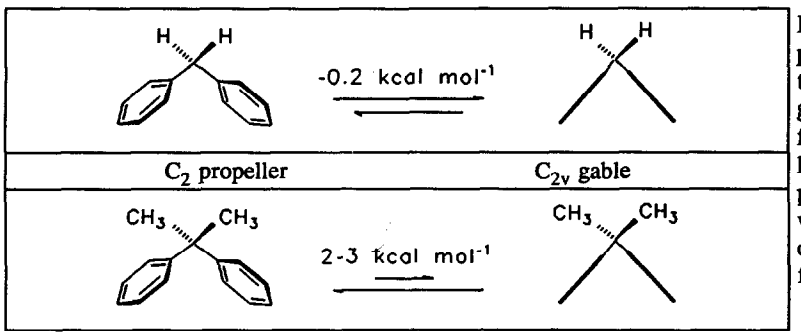


**FIGURE 2.** (Upper) Diphenylmethane conformations, with the $C_{2v}$ gable geometry being slightly favored over the $C_2$ propeller. (Lower) 2,2-Diphenylpropane conformations, with the $C_2$ propeller geometry more substantially favored.

In the tetrapyrrole analogs (**1** and **2**) of 2,2-diphenylpropane and diphenylmethane, respectively, the longer dipyrrinone blades have at least one degree of conformational freedom not available in the simpler systems: the potential for curvature within the blades by twisting the C(5)-C(6) or C(14)-C(15) carbon-carbon single bonds. However, the conformational possibilities within the dipyrrinone blades are severely limited, as judged from earlier work involving both experiment[3] and CNDO/2-based force field calcula-

tions,[3,10] which indicate a strong preference for the *syn*-periplanar or *syn*-clinal conformations. The *syn*-periplanar conformation with C(5)-C(6) or C(14)-C(15) torsion angles 0-20° predominates in crystalline bilirubin, and in dipyrrinone hydrogen-bonded *dimers*. *Syn*-clinal conformations, with C(5)-C(6) torsion angles 20-50° are favored by *monomeric* dipyrrinones with unsubstituted N-H groups. In bilirubins, differences in shape brought about by twisting the blades are small compared with conformations generated through rotations of the dipyrrinone blades about their C(9)-C(10) and C(10)-C(11) bonds.

Rotations about the C(9)-C(10) and C(10)-C(11) carbon-carbon single bonds sweep the dipyrrinone blades through large spatial distances and produce a wide variety of rather different and distinctive conformational structures. At the two extremes are the planar or nearly planar porphyrin-like and extended conformations of Fig. 1. (The porphyrin-like conformation is designated the $\phi_1=\phi_2\simeq 0°$ conformer; the extended conformation can be designated the $\phi_1=\phi_2\simeq 180°$ conformer.) Lying in between these two planar conformations are a very large number of non-planar conformations, each of which has a non-superimposable mirror image (as in the $\phi_1=\phi_2=90°$ and $\phi_1=\phi_2=-90°$ gabled conformers). However, not all of the conformers are expected to be equal in energy.[3,4,10] For example, in the extended conformation ($\phi_1=\phi_2=180°$) the propionic acid groups are severely buttressed against one another; and in the porphyrin-like conformation ($\phi_1=\phi_2=0°$) destabilizing non-bonded steric interactions arise between the pyrrole N-H groups and the lactam carbonyl groups. These two conformers (Fig. 1A and 1B) might thus be expected to be less stable than any of the non-planar conformations in which non-bonding repulsions are minimized.

An examination of CPK-space filled models allows one to see the cited elements of conformational destabilization, and molecular mechanics force field calculations place those observations on a quantitative basis. Using the SYBYL force field program on an Evans and Sutherland ESV-10 graphics workstation, conformational energy maps for **1** and **2** were generated (Figs. 3 and 4). The maps are similar, but for **2** it is essentially devoid of local minima; whereas, for **1** there are clearly separated local minima apparently representing conformations imposed on the molecule by the *gem*-dimethyl effect. In both maps, isoenergetic global minima are clearly located near ($\phi_1=\phi_2\simeq 60°$), ($\phi_1=\phi_2\simeq -60°$), ($\phi_1=\phi_2\simeq 300°$), ($\phi_1\simeq 300°$, $\phi_2\simeq -60°$), and ($\phi_1\simeq -60°$, $\phi_2\simeq 300°$). Each global minimum lies as a deep depression in a canyon with steeply rising walls. Interestingly, even in the absence of hydrogen bonding the minimum-energy conformation places the propionic acid carboxyl groups in a position ideal for hydrogen bonding to the opposing dipyrrinone lactam carbonyl and N-H groups and the pyrrole N-H group. But hydrogen bonding sharply lowers the global energy minima and thus acts as a powerful conformation-stabilizing force — not available to most of the other tetrapyrrole conformers which form the conformational energy map.

The global minimum conformations of Figs. 3 and 4 correspond to either of two unique 3-dimensional conformers, ***M*** and ***P*** (Fig. 5) which appear to play a central role in explaining many of the properties of the pigments. Interestingly for bilirubin itself, the global minimum ridge-tile conformers found in our force field calculations are nearly identical to those seen in X-ray crystal structures of bilirubin[5a-d] and its analogs in which the vinyl groups are replaced by ethyl (mesobilirubin).[5e] In those conformations (Fig. 1C), the polar propionic acid carboxyl groups are sequestered internally, thus rendering the pigment lipophilic. It may be seen that the ***M*** and ***P*** conformers of Fig. 5 are mirror image structures: ***P*** corresponds to the global minimum (Fig. 3 or 4) at ($\phi_1=\phi_2\simeq 60°$), ***M*** corresponds to global minima at ($\phi_1=\phi_2\simeq -60°$), ($\phi_1=\phi_2\simeq 300°$), ($\phi_1\simeq -60°$, $\phi_2\simeq 300°$) and ($\phi_1\simeq 300°$, $\phi_2\simeq -60°$). The ***M*** and ***P*** conformational enantiomers interconvert by breaking the minimum number of hydrogen bonds while rotating the dipyrrinones about $\phi_1$ and $\phi_2$ and remaking the hydrogen bonds. From an examination of Figs. 3 and 4 two distinct low energy

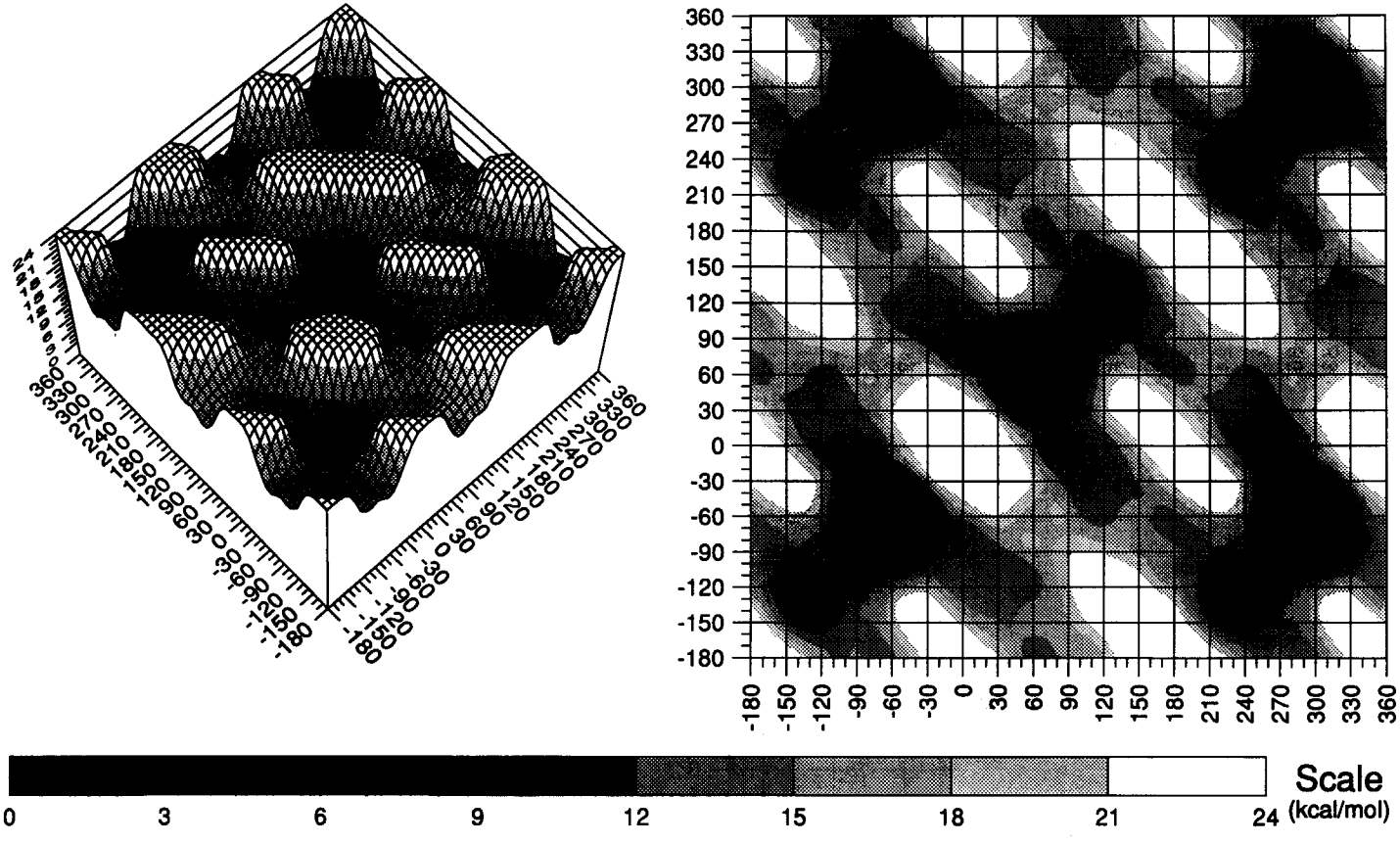


**FIGURE 3.** Potential energy surface (Left) and contour map (Right) for 10,10-dimethylglaucorubin (**1**) conformations generated by rotating the two dipyrrinone groups independently about the C(9)-C(10) and C(10)-C(11) bonds ($\phi_1$ and $\phi_2$ respectively). The energy scale (Bottom) is in kcal/mol. Isoenergetic global minima (set to 0 kcal/mol) are found near ($\phi_1$,$\phi_2$) = (60°,60°) (***P***-chirality) and near ($\phi_1$,$\phi_2$) = (-60°,-60°), (-60°,300°), (300°, -60°), (300°, 300°) (***M***-chirality). Local minima (7 kcal/mol above the global minima) are found near ($\phi_1$,$\phi_2$) = (120°, 120°), (-120°, -120°), (-120°, 240°), (240°, -120°) and (240°, 240°). Data are from molecular dynamics simulations using SYBYL® (Tripos assoc.) on an Evans & Sutherland ESV-10 workstation. The energy surface display was created using Wingz™ (Informix).

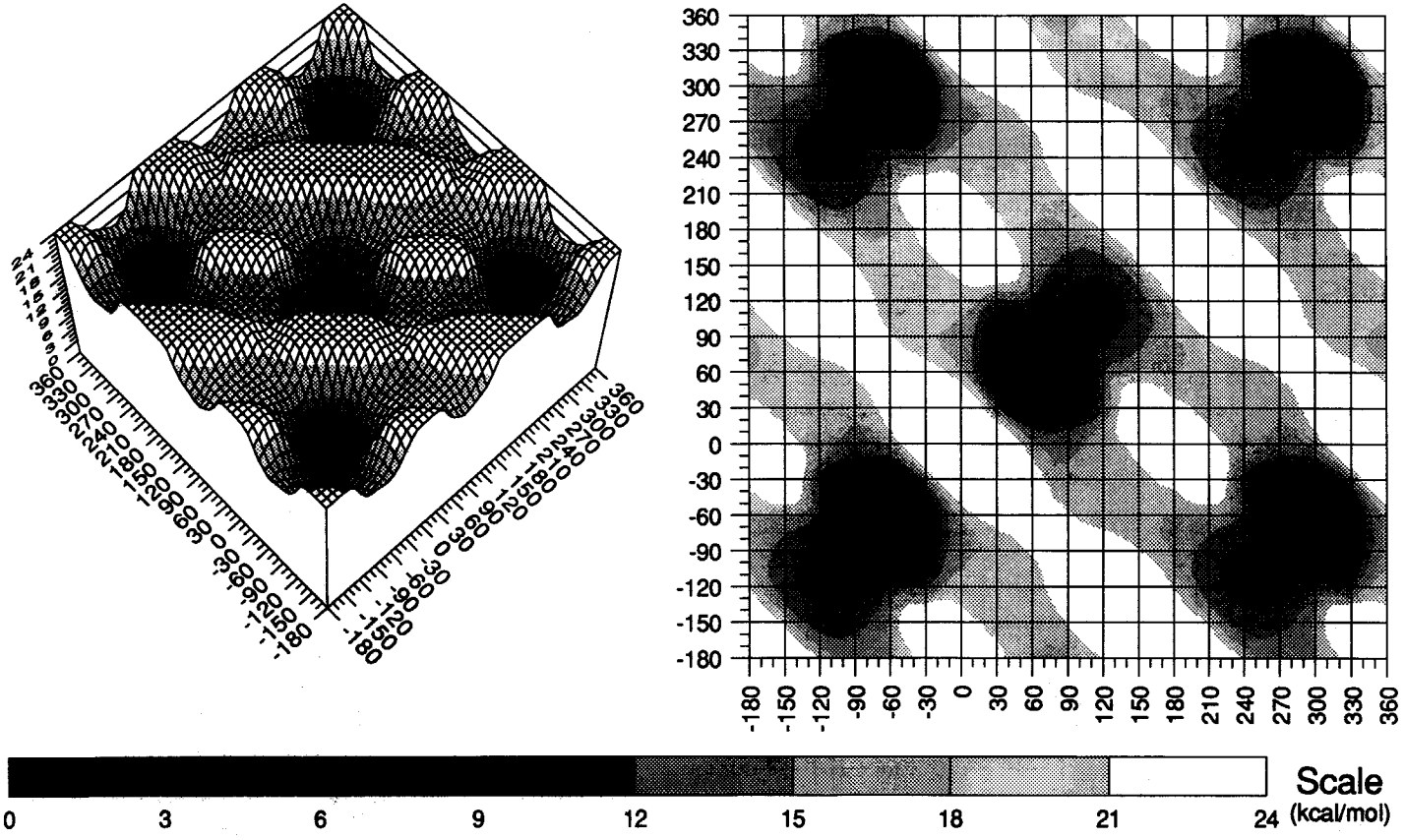


**FIGURE 4.** Potential energy surface (Left) and contour map (Right) for glaucorubin (**2**) conformations generated by rotating the two dipyrrinone groups independently about the C(9)-C(10) and C(10)-C(11) bonds ($\phi_1$ and $\phi_2$ respectively). The energy scale (Bottom) is in kcal/mol. Isoenergetic global minima (set to 0 kcal/mol) are found near ($\phi_1$,$\phi_2$) = (60°,60°) (***P***-chirality) and near ($\phi_1$,$\phi_2$) = (-60°,-60°), (-60°,300°), (300°, -60°), (300°, 300°) (***M***-chirality). Local minima (9 kcal/mol above the global minima) are found near ($\phi_1$,$\phi_2$) = (110°, 110°), (-110°, -110°), (-110°, 250°), (250°, -110°) and (250°, 250°). Data are from molecular dynamics simulations using SYBYL® (Tripos assoc.) on an Evans & Sutherland ESV-10 workstation. The energy surface display was created using Wingz™ (Informix).

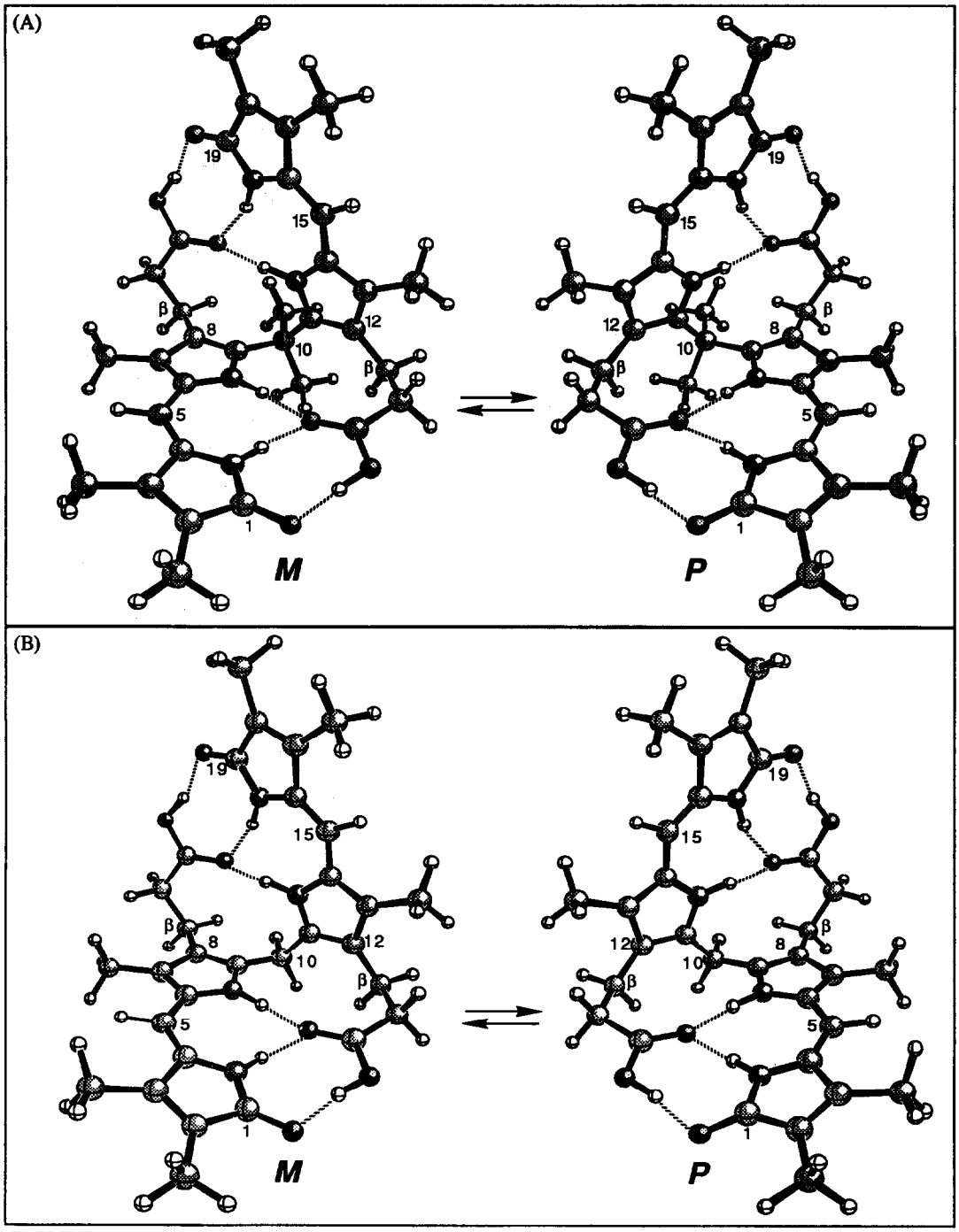


**FIGURE 5.** Ball and stick conformational representations for ridge-tile shape *M* and *P* chirality intramolecularly hydrogen-bonded interconverting enantiomers of (A) 10,10-dimethylglaucorubin (**1**) and (B) glaucorubin (**2**). The conformers correspond to the global energy minimima identified in Figs. 3 and 4.

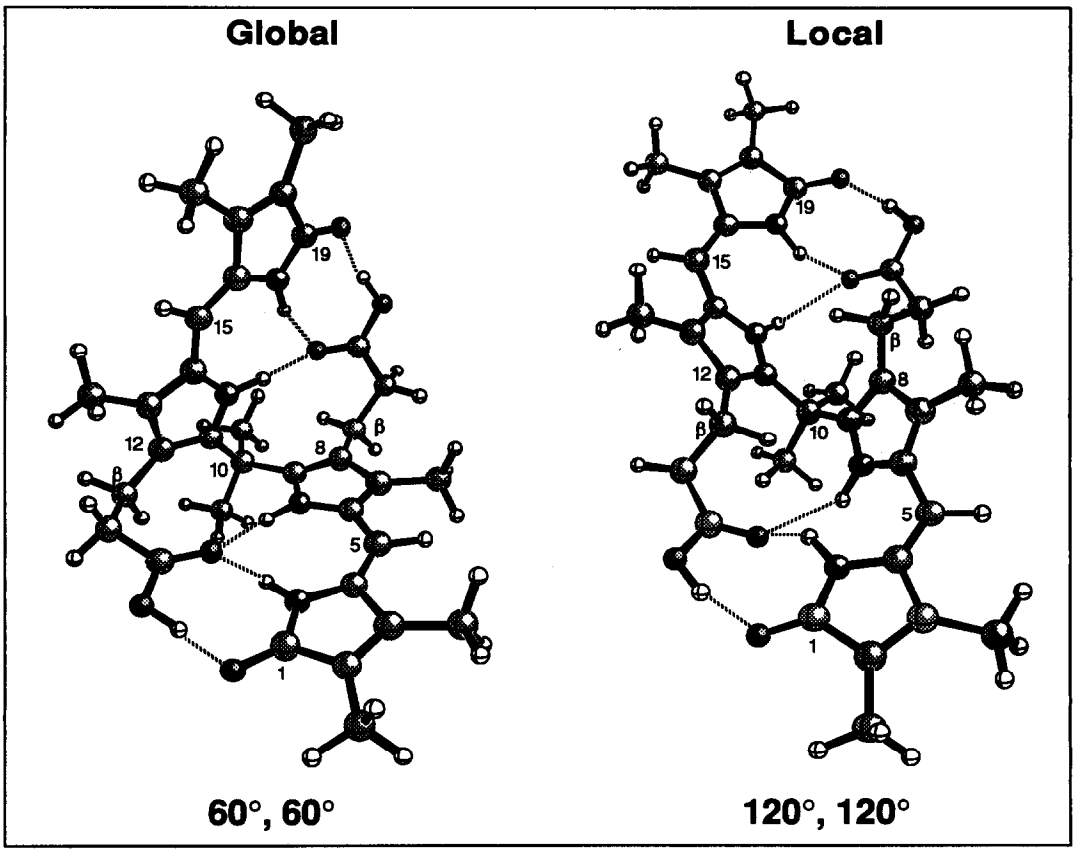


**FIGURE 6.** Ball and stick conformations of *P*-chirality 10,10-dimethylglaucorubin (**1**) at the global (left) and local (right) minima. The local minimum latter lies ~7 kcal/mole above the global.

interconversion pathways may be charted from *P* to *M*: (1) a route from ($\phi_1=\phi_2\simeq 60°$) → ($\phi_1\simeq 0°$, $\phi_2\simeq 90°$) → ($\phi_1\simeq -30°$, $\phi_2\simeq 90°$) → ($\phi_1\simeq -60°$, $\phi_2\simeq 60°$) → ($\phi_1\simeq -90°$, $\phi_2\simeq 30°$) → ($\phi_1\simeq -90°$, $\phi_2\simeq 0°$) and down to ($\phi_1=\phi_2\simeq -60°$), with an activation barrier of ~17 kcal/mole in the case of **1** and ~22 kcal/mole in the case of **2**. (2) A route from ($\phi_1=\phi_1\simeq 60°$) → ($\phi_1\simeq 0°$, $\phi_2\simeq 90°$) → ($\phi_1\simeq -30°$, $\phi_2\simeq 120°$) → ($\phi_1\simeq -60°$, $\phi_2\simeq 180°$) → ($\phi_1\simeq -90°$, $\phi_2\simeq 210°$) → ($\phi_1\simeq -90°$, $\phi_2\simeq 240°$) and down to ($\phi_1\simeq -60°$, $\phi_2\simeq 300°$), with a barrier of ~15 kcal/mole in the case of **1** and ~19 kcal/mole in the case of **2**.

The high energy valleys (or non-isolated local minima) protruding from the global minima of **2** (Fig. 4) appear to separate and drop in energy, becoming clearly defined local minima in the *gem*-dimethyl analog **1** (Fig. 3). Structures at the global and local minima of **1** are compared in Fig. 6. Like the global minimum, the local minimum conformation is also stabilized by intramolecular hydrogen bonds, accommodated by the dipyrrinones twisting out of planarity. The latter is accommodated by rotations in the propionic acid chain that bring the $\beta$-$CH_2$ groups forward (required at some point along the $P \rightleftarrows M$ interconversion path),[11] and by slight twisting about C(5)-C(6) and C(14)-C(15) in the dipyrrinones. Nonbonded steric repulsions involving the *gem*-dimethyls are thus somewhat relieved at the expense of longer (less stable) hydrogen bonds. Further evidence for intramolecular hydrogen bonding may be found from $^1$H-NMR studies.

**Conformation from NMR.** Conformation-determining intramolecular hydrogen bonding in **1** and **2** is clearly revealed by $^1$H-NMR spectroscopy. Previous studies of bilirubin pigments have shown that the pyrrole and lactam N-*H* chemical shifts are an excellent probe for determining whether the dipyrrinone units of a bilirubin molecule are involved in *intra*molecular hydrogen bonding.[6,12] Thus, in $CDCl_3$ solvent the pyrrole N-*H* chemical shift typically appears near 9.2 $\delta$, the lactam N-*H* near 10.6 $\delta$ and the $CO_2H$ near 13.6 $\delta$, when the pigment adopts an intramolecularly hydrogen bonded state (as in Fig. 1C). In $(CD_3)_2SO$ solvent, which strongly hydrogen bonds to the pigment, the pyrrole N-*H* resonance becomes more deshielded (to ~10.3 $\delta$) while the lactam N-*H* and propionic $CO_2H$ resonances become more shielded (to ~9.7 and 11.9 $\delta$, respectively). As shown in Table 1, although the N-*H* and $CO_2H$ resonances of **1** and **2** are similar in $CDCl_3$ and in $(CD_3)_2SO$, there are important differences. As might be expected, the chemical shifts of **2** are essentially identical to those of mesobilirubin-XIII$\alpha$ (the 3,17-diethyl analog of **2**),[9] which is believed to adopt a ridge-tile hydrogen-bonded structure (as in Fig. 1C) in $CDCl_3$.[4,6] In contrast, the lactam N-*H* resonances of **1** are more deshielded (than those of **2**) by ~0.5 ppm and the pyrrole N-*H* resonances are more shielded by ~0.25 $\delta$. These data suggest somewhat stronger hydrogen bonding between the $CO_2H$ and lactam —NH—C=O of **1** than in **2**, and less effective hydrogen bonding to the pyrrole N-*H* of **1**. These changes in shieldings may be attributed to a change in the conformation of **1** (relative to **2**) — forced by accommodation of the *gem*-dimethyls. One is tempted to assume a somewhat flatter ridge-tile conformation for **1** than for **2** (an average of the conformations shown in Fig. 6).

**TABLE 1.** Comparison of 10,10-Dimethylglaucorubin (**1**), Glaucorubin (**2**) and Mesobilirubin-XIII$\alpha$ (MBR-XIII) Lactam and Pyrrole N-*H* Chemical Shifts[a] in $CDCl_3$ and $(CD_3)_2SO$ Solvents.[b]

| Pigment | $\delta_H$ in $CDCl_3$ | | | $\delta_H$ in $(CD_3)_2SO$ | | |
|---|---|---|---|---|---|---|
| | Lactam | Pyrrole | $CO_2H$ | Lactam | Pyrrole | $CO_2H$ |
| **1** | 11.08 | 8.91 | 13.93 | 9.48 | 10.13 | 11.90 |
| **2** | 10.61 | 9.15 | 13.59 | 9.78 | 10.32 | 11.89 |
| MBR-XIII[c] | 10.57 | 9.15 | 13.62 | 9.74 | 10.28 | 11.87 |

[a] $\delta$, ppm downfield from $(CH_3)_4Si$; [b] Run as $10^{-2}$ *M* $(CD_3)_2SO$ and $10^{-3}$ *M* $CDCl_3$ solutions at 22°C. [c] Data from references 8 and 9.

In contrast, in $(CD_3)_2SO$ solvent, where all of the dipyrrinone N-*H*s become hydrogen-bonded to sulfoxide, the lactam N-*H*s shift to ~9.7 $\delta$, the pyrrole N-*H*s to ~10.3 $\delta$ and the $CO_2H$s to ~11.9 $\delta$. Although the distinctions due to intramolecular hydrogen bonding (in $CDCl_3$) are lost, the slightly more shielded N-*H*s in **1** could be attributed to slightly less effective hydrogen bonding to sulfoxide solvent due to an altered pigment conformation.

Analysis of the vicinal H | H coupling constants in the propionic acid chains of **1** and **2** (Table 2) provides direct experimental evidence for folded (ridge-tile) structures (Figs. 5 and 6). The well-defined ABCX pattern seen in $CDCl_3$ is characteristic of a less mobile conformation;[6] whereas, the less complicated $A_2B_2$ pattern in $(CD_3)_2SO$ [**1**: 2.19 (2H, t, J=7.8 Hz) and 1.98 (2H, t, J=7.8 Hz); **2**: 2.41 (2H, t, J=7.8 Hz); 1.92 (2H, t, J=7.8 Hz)] indicates considerably greater conformational mobility in the $-CH_AH_XCH_BH_CCO_2H$ segment. In $CDCl_3$ **1** and **2** adopt a conformation where the propionic acid residues are constrained to adopt fixed staggered geometry (Table 2); whereas in $(CD_3)_2SO$ no such constraint

is evident. However, even in the fixed staggered geometry of the propionic acid residue, only minor differences in the Karplus equation-determined[13] H-C-C-H torsion angles ($\omega$, Table 2) can be detected for **1** and **2**. Whatever differences might obtain for the relative orientations of the dipyrrinones of **1** and **2**, such differences are not easily detected by the coupling constant/torsion angle analysis.

**TABLE 2.** $^1$H-NMR Chemical Shifts,[a] Coupling Constants (J, Hz) and H-C-C-H Torsion Angles ($\omega$) for the Propionic Acid $-CH_AH_XCH_BH_CCO_2H$ Segment in $CDCl_3$ at 22°C.

| Pig-ment | $H_A$ | $H_B$ | $H_C$ | $H_X$ | Fixed Staggered Geometry of Propionic Segments |
|---|---|---|---|---|---|
| **1** | 3.5 $\delta$ | 2.93 $\delta$ | 2.78 $\delta$ | 2.55$\delta$ | 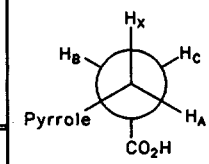 |
| $\omega^b$ | ($J_{AB}$ 11.5,$J_{AC}$ 3.1,$J_{AX}$-13.0) $\omega_{AC}$=58° | ($J_{BC}$-18.5,$J_{BX}$ 2.6) $\omega_{BX}$=62° | ($J_{CX}$ 4.7) $\omega_{CX}$=49° | | |
| **2** | 2.99 $\delta$ | 2.89 $\delta$ | 2.78 $\delta$ | 2.54 $\delta$ | |
| $\omega^b$ | ($J_{AB}$ 13.5,$J_{AC}$ 2.8,$J_{AX}$-15.0) $\omega_{AC}$=60° | ($J_{BC}$-18.7,$J_{BX}$ 2.6) $\omega_{BX}$=62° | ($J_{CX}$ 4.6) $\omega_{CX}$=49° | | |



[a] Chemical shifts in ppm downfield from $(CH_3)_4Si$. [b] From $^3J = 9.3\cos^2\omega + \cos\omega$, see reference 13.

The stereochemical conclusions reached above are confirmed by $^1$H-NMR NOE measurements (Table 3). In both **1** and **2**, the *syn-Z* dipyrrinone conformation is confirmed by moderately strong NOEs between i) the vinylic protons at C(5) and C(15) and the methyls at C(3), C(7), C(13) and C(17), and ii) the pyrrole and lactam NHs. Significantly, NOEs are observed between the $\beta$-$CH_2$ ($H_A$) and the C(10) *gem*-dimethyls in **1**, and between ($H_B$) and the C(7) and C(13) $CH_3$ groups in both **1** and **2** — as might be expected from the conformations shown in Figs. 5 and 6. Intramolecular hydrogen bonding between the COOH group and the dipyrrinone NHs is also supported by NOEs: in **2** a stronger NOE is seen between the pyrrole NH and COOH than in **1**, in accord with the earlier suggestion that the relatively more shielded pyrrole N-H of **1** is due to a weaker or longer hydrogen bond than in **2**. Some of the most significant NOE data in $CDCl_3$ for **1** and **2** are absent in $(CD_3)_2SO$ solvent, and thus the clear support for intramolecularly hydrogen-bonded conformations for **1** and **2** in $CDCl_3$ is lost in $(CD_3)_2SO$ solvent.

The data of Tables 1-3 support a fixed staggered conformation for the propionic acid segment in $CDCl_3$ and thus indicate that the conformational enantiomer equilibria represented in Fig. 5 are slow on the NMR time scale. The coalescence temperature for $-CH_AH_XCH_BH_CCO_2H$ was determined to be 55°C for **1** in $CDCl_3$ or $(CDCl_2)_2$ solvent; whereas, for **2** in $(CDCl_2)_2$, it was 95°C. The latter is in good agreement with the coalescence temperature (95°C) determined for bilirubin and mesobilirubin-XIII$\alpha$,[6] but it is much higher than that of **1**. Since an increased conformational mobility in the propionic acid group is expected to attend the conformational inversion shown in Fig. 5, the lower coalescence temperature for **1** correlates well with its computed (Fig. 3) lower activation barrier as compared with **2** (Fig. 4). Analysis (Eyring equation) of the temperature-dependence of propionic acid segment coalescence gives conformational inversion

barriers of 18 and 21 kcal/mole for **1** and **2**, respectively — in good agreement with the 15-17 kcal/mole and 19-22 kcal/mole barriers computed for **1** and **2**, respectively by molecular dynamics.

**TABLE 3.** Nuclear Overhauser Enhancements (NOE) of Selected Protons in 10,10-Dimethylglaucorubin (**1**) and Glaucorubin (**2**) in $CDCl_3$ and $(CD_3)_2SO$ at 22°C.

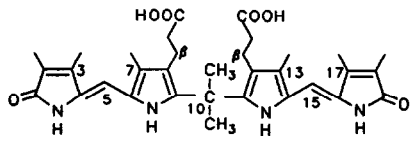


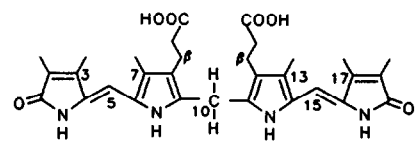


| Irradiated Proton | NOE in $CDCl_3$ Solvent for | | NOE in $(CD_3)_2SO$ Solvent for | | Observed Proton |
|---|---|---|---|---|---|
| | 1 | 2 | 1 | 2 | |
| C(5,15)=CH | 4% | 4% | 4% | 4% | C(7,13) -$CH_3$ |
| C(5,15)=CH | 4% | 4% | 4% | 4% | C(3,17) -$CH_3$ |
| Pyrrole NH | 4% | 4% | 4% | 4% | Lactam NH |
| β-$CH_2$ ($H_A$) | 8% | — | < 0.1% | — | C(10)$(CH_3)_2$ |
| β-$CH_2$ ($H_A$) | — | < 0.1% | — | < 0.1% | C(10) $CH_2$ |
| C(10)$(CH_3)_2$ | 3% | — | < 0.1% | — | β-$CH_2$ |
| C(10)$CH_2$ | — | < 0.1% | — | < 0.1% | β-$CH_2$ |
| β-$CH_2$ ($H_B$) | 3% | 3% | — | — | C(7,13) -$CH_3$ |
| Pyrrole NH | < 0.1% | 1% | < 0.1% | < 0.1% | COOH |
| Lactam NH | 3% | 3% | < 0.1% | < 0.1% | COOH |
| COOH | 3% | 3% | < 0.1% | < 0.1% | Lactam NH |

***Conformational Enantiomerism and Induced Circular Dichroism.*** In a non-polar, aprotic solvent such as dichloromethane, the conformational equilibrium between bilirubin enantiomers can be displaced from 1:1 by the addition of a chiral recognition agent.[14] Similarly, for bilirubin analogs **1** and **2** an induced CD may be observed in the presence of quinine (Fig. 7). At a mole ratio of alkaloid:pigment of ~300:1, the Cotton effect intensities reach a maximum for glaucorubin (**1**), giving an intense bisignate CD ($\Delta\epsilon^{max}_{429}$ -145, $\Delta\epsilon^{max}_{384}$ +74), of exactly the same signed order and nearly the same magnitude as that seen for bilirubin or mesobilirubin-XIIIα.[14] With 10,10-dimethylglaucorubin (**1**), however, the Cotton effect intensities are reduced by nearly an order of magnitude ($\Delta\epsilon^{max}_{443}$ -22, $\Delta\epsilon^{max}_{392}$ +21). Whether this reflects ineffective complexation/recognition or an altered pigment conformation is not immediately clear. However, it is clear that although **2** behaves qualitatively like **1**, it does not behave exactly like **1** — again further evidence that the *gem*-dimethyls group exerts an important stereochemical effect. In contrast, $2x10^{-5}$ *M* solutions of **1** and

2 in dichloromethane containing 2.0 *M* *R*-(+)-methyl-*p*-tolylsulfoxide show essentially identical CD curves with much weaker Cotton effects: **1** ($\Delta\epsilon_{435}^{max}$ +14.6, $\Delta\epsilon_{389}^{max}$ -8.5, λ (at $\Delta\epsilon$=0) 408 nm) and **2** ($\Delta\epsilon_{436}^{max}$ +11.5, $\Delta\epsilon_{391}^{max}$ -6.2, λ (at $\Delta\epsilon$=0) 404 nm). These data suggest that the conformation of **1** and **2** is essentially identical in the presence of sulfoxide,[15] *e.g.*, as suggested by $^1$H-NMR studies in $(CD_3)_2SO$ (Tables 1-3).

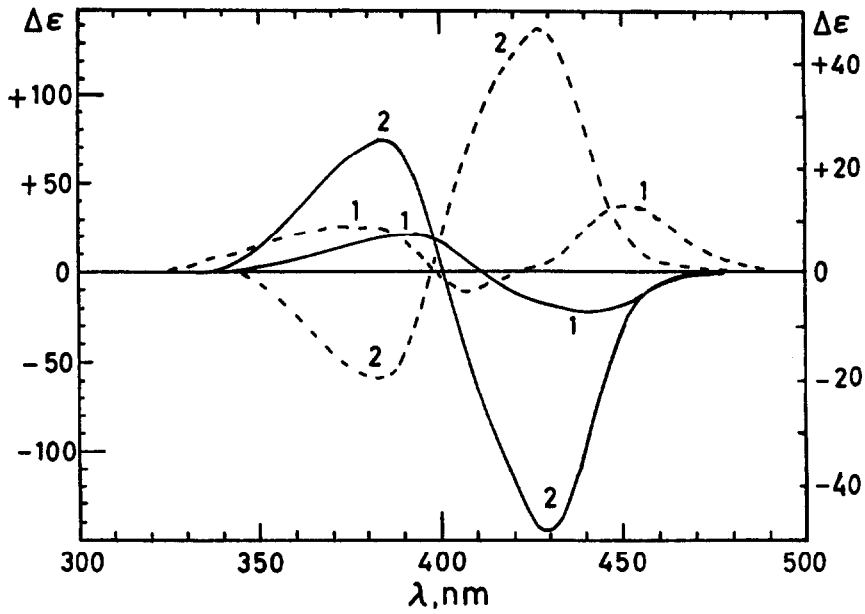


**FIGURE 7.** Circular dichroism spectra of 2.0 x$10^{-5}$ *M* 10,10-dimethylglaucorubin (**1**) and Glaucorubin (**2**) in $CH_2Cl_2$ in the presence of 6.0 x$10^{-3}$ *M* quinine at 22°C (——, read $\Delta\epsilon$ on left vertical axis). Circular dichroism spectra of 2.5 x$10^{-5}$ *M* **1** and **2** in pH 7.4 aq. Tris buffer containing 5.0 x$10^{-5}$ *M* human serum albumin (HSA) at 22°C (- - - -, read $\Delta\epsilon$ on right vertical axis). The spectra were recorded within 15 min after preparation of the solution and remained essentially invarian for 24 h at 22°C. A CD spectrum of the same concentration of **1** or **2** without added quinine or HSA falls on the $\Delta\epsilon$=0 line.

However, when human serum albumin (HSA) is used as the chiral complexation agent, aqueous solutions (pH 7.4 buffered) of **2** behave very similarly to those of bilirubin or mesobilirubin-XIII$\alpha$,[16] exhibiting moderately intense bisignate CD curves ($\Delta\epsilon_{429}^{max}$ +56, $\Delta\epsilon_{384}^{max}$ -24) due to enantioselective chiral complexation of the pigment by the protein. For solutions of **1** with HSA, however, the CD is considerably altered ($\Delta\epsilon_{451}^{max}$ +13, $\Delta\epsilon_{408}^{max}$ -3.5, $\Delta\epsilon_{372}^{max}$ +9.1) with no clearly defined bisignate shape. The data indicate that the conformation of **1** on HSA is probably rather different from that of **2** on HSA, but just how different and in what way different is difficult to assess at present.

When the chiral agent is covalently attached to the pigment, as in propionamide derivatives with amino acid esters, CD may also be observed. Thus, following conversion of **1** and **2** to their bis-amides (**3** and **4**, respectively) with *S*-alanine methyl ester by the Shioiri procedure used previously,[17] the CD spectra of the optically active pigment amides were determined (Fig. 8). Not surprisingly, a moderately strong bisignate CD curve is found for **4**, but unexpectedly, only a very weak CD is found for **3** in the organic solvents studied (Table 4). The data suggest very weak conformational selection of the *P*-helicity

diastereomer in **3**, but an order of magnitude stronger selection of the *P*-helicity diastereomer in **4**. Interestingly, although $^1$H-NMR (in which the propionamide (*HN*-C=O) is found to be strongly deshielded) indicates a high probability of intramolecular hydrogen bonding in **4** (Table 5), the propionamide (HN-C=O) group of **3** *appears not to be involved in hydrogen bonding*. Thus, it would seem that whereas the conformation of **4** retains its hydrogen bonded ridge-tile structure, the conformation of **3** is not quite the same. Clearly, the C(10) *gem*-dimethyl group plays a major role in apparently detering intramolecular hydrogen bonding in the bis-amide (**3**) but apparently not in the parent diacid (**1**). The reasons for the difference in behavior are not entirely clear, but they may relate to the longer length of the O-H *vs* N-H bond in a more open ridge-tile conformation (in **3** and **1**) *vs* that of **4** and **1**, where intramolecular hydrogen bonding is accessible in both the acid and amide.

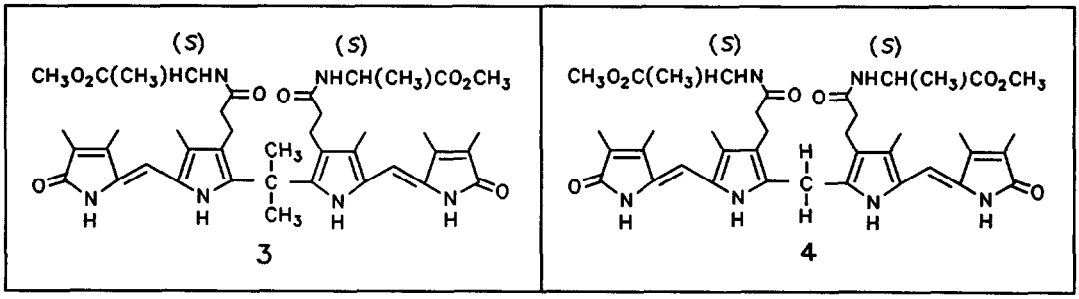


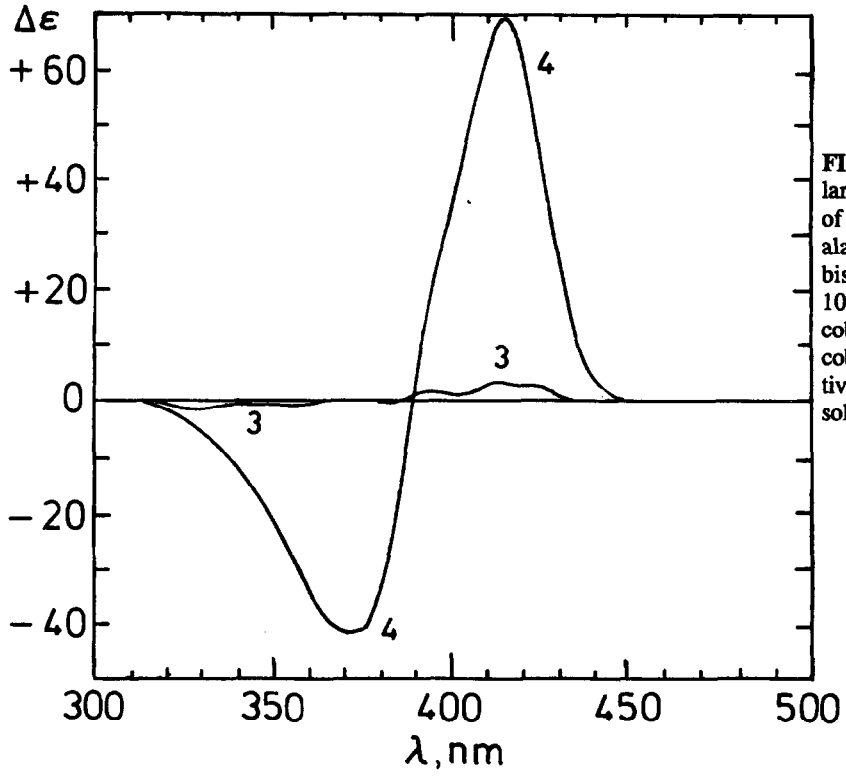


**FIGURE 8.** Circular dichroism spectra of 1.0 x$10^{-5}$ *M* (S)-alanylmethyl ester bis-amides **3** and **4** of 10,10-dimethylglaucobilin (**1**) and glaucobilin (**2**), respectively, in $CH_3CN$ solvent at 22°C.

**TABLE 4.** Circular Dichroism and UV-Visible Spectral Data[a] for the Bis-Amides (3 and 4) of 10,10-Dimethylglaucorubin (1) and Glaucorubin (2) with *S*-Alanine Methyl Ester in Organic Solvents at 22°C.

| Solvent | Pigment | Circular Dichroism | | | UV-Visible |
|---|---|---|---|---|---|
| | | $\Delta\epsilon_{max}$ ($\lambda_1$) | $\lambda$ at $\Delta\epsilon$=0 | $\Delta\epsilon_{max}$ ($\lambda_2$) | $\epsilon_{max}$ ($\lambda$) |
| $CH_2Cl_2$ | 3 | +1.2 (414) | 390 | -2.3 (375) | 38,000 (420) |
| | 4 | +32 (415) | 388 | -20 (375) | 41,400 (406) |
| $CH_3CN$ | 3 | +3.5 (412) | 390 | -1.0 (375) | 36,000 (417) |
| | 4 | +69 (414) | 387 | -41 (373) | 43,000 (414) |
| $(CH_3)_2CO$ | 3 | +3.2 (412) | 388 | -1.0 (375) | 39,000 (416) |
| | 4 | +67 (416) | 388 | -39 (374) | 36,500 (416) |
| $CH_3OH$ | 3 | +1.9 (419) | 390 | +0.5 (380) | 37,500 (421) |
| | 4 | +52 (420) | 390 | -28 (380) | 46,000 (418) |
| $(CH_3)_2SO$ | 3 | +0.5 (422) | — | — | 39,500 (427) |
| | 4 | +10 (420) | 389 | -1.7 (379) | 47,000 (425) |

[a]$\Delta\epsilon$ and $\epsilon$ in L · mole$^{-1}$ · cm$^{-1}$ and $\lambda$ in nm; [b]For 1 x10$^{-5}$ *M* pigment solutions.

**TABLE 5.** $^1$H-NMR Chemical Shifts*a* of Amide and Pyrrole N-*H*'s of the *S*-Alanine Methyl Ester Bis-amides (3 and 4) of 10,10-Dimethylglaucorubin (1) and Glaucorubin (2), in $CDCl_3$ at 22°C.

| Pigment | $\delta$ (N-*H*) ppm | | |
|---|---|---|---|
| | Lactam | Pyrrole | Alanine |
| 3 | 10.41 | 8.97 | 7.30 (syn)<br>6.12 (anti) |
| 4 | 11.70 | 10.62 | 10.25 (syn) |

[a]$\delta$, ppm downfield from $(CH_3)_4Si$.

## CONCLUDING COMMENTS

Intramolecular hydroben bonding between the propionic acid $CO_2H$ and dipyrrinone groups is known to be a dominant, conformation-stabilizing force in bilirubin. In the current study, the influence of a *gem*-dimethyl group at C(10) in a bilirubin analog is evaluated. The *gem*-dimethyl effect introduces an internal steric buttressing on the propionic acid chains that somewhat destabilizes the original intramolecularly hydrogen bonded ridge-tile conformation, rendering amphiphilic 10,10-dimethylglaucorubin (1) more soluble in both polar and non-polar organic solvents than either the parent glaucorubin (2) or bilirubin. The gem-dimethyls appear to force a flatter ridge-tile shape in 1, as compared with 2, thus stabilizing a new conformation wherein the dihedral angle (shown in Fig. 1C) is larger and the dipyrrinones are twisted so as to retain hydrogen bonding — as in Fig. 6. This conformation may be important in its dictating solution and

spectroscopic properties. The *gem*-dimethyl effect thus represents a new way to perturb the conformation and hence the properties of intramolecularly hydrogen-bonded bilirubin pigments by judiciously targeting apparently remote substitution in order to achieve an allosteric effect.

## EXPERIMENTAL

**General Procedures.** All ultraviolet-visible spectra were recorded on a Perkin-Elmer 3840 diode array or Cary 219 spectrophotometer, and all circular dichroism (CD) spectra were recorded on a JASCO J-600 instrument. The CD and UV-vis solutions were prepared as described previously.[13-16] Nuclear magnetic resonance (NMR) spectra were determined on a GE QE-300 300-MHz spectrometer in $CDCl_3$ solvent (unless otherwise specified) and reported in $\delta$ ppm downfield from $(CH_3)_4Si$. Melting points were determined on a Mel-Temp capillary apparatus and are uncorrected. Combustion analyses were carried out by Desert Analytics, Tucson, AZ. Analytical thin layer chromatography was carried out on J.T. Baker silica gel IB-F plates (125 $\mu$ layers). Flash column chromatography was carried out using Woelm silica gel F, thin layer chromatography grade.

Spectral data were obtained in spectral grade solvents (Aldrich or Fisher). Diphenylphosphonylazide, triethylamine and dimethylsulfoxide were from Aldrich. *S*-(+)-Alanine methyl ester hydrochloride was from Sigma.

**10,10-Dimethyl-3,17-bis-nor-mesobilirubin-XIII$\alpha$ (10,10-Dimethylglaucorubin) (1).** This pigment was prepared by total synthesis, as previously described.[8]

**3,17-Bis-nor-mesobilirubin-XIII$\alpha$ (Glaucorubin) (2).** This pigment was prepared by total synthesis, as previously described.[8]

**10,10-Dimethylglaucorubin Bis-amide with *S*-alanine methyl ester (3).** 10,10-Dimethylglaucorubin (1) (14.7 mg, 0.025 mmole), *S*-(+)-alanine methyl ester hydrochloride (35 mg, 0.25 mmole), diphenylphosphoryl azide (28 mg, 0.25 mmole) and triethyl amine (51 mg, 0.5 mmole) were mixed in 0.5 mL of dry dimethyl sulfoxide at room temperature. The mixture was stirred in the dark for 20 hours. To the yellow cloudy solution was added 20 mL of dichloromethane, and the solution was washed with water (3 x10 mL). Then the dichloromethane solution was flash chromatographed on a short column (TLC grade silica gel deactivated with 15% water). Elution with dichloromethane (100 mL) removed unreacted azide and amines. The bis-amide was then eluted with dichloromethane/methanol (50:1) (100 mL). Evaporation of solvent and drying afforded 10.6 mg of the bis-amide (56% yield). It had mp 115-117°C; $[\alpha]_D^{25}$ = -37° (*c* 0.02, $CH_2Cl_2$); IR (deposition from $CH_2Cl_2$) $\nu$: 3410, 1725, 1645, 1545 $cm^{-1}$; $^1$H-NMR ($CDCl_3$) $\delta$: 1.21 (d, 6H, J=7 Hz), 1.86 (s, 6H), 1.87 (s, 6H), 2.07 (s, 6H), 2.10 (s, 6H), 2.47 (m, 8H), 3.66 (s, 3H), 4.53 (q, 2H), 6.07 (s, 2H), 6.12 (d, *trans*-CONH, J=7 Hz), 7.30 (d, *cis*-CONH, J=7 Hz), 8.97 (broad, 2NH), 10.41 (broad, 2NH) ppm.

*Anal.* Calcd. for $C_{41}H_{54}N_6O_8$ (767): C, 64.88; H, 7.26; N, 10.82
Found: C, 64.11; H, 7.07; N, 10.41

**Glaucobilin Bis-amide with *S*-alanine methyl ester (4).** Glaucobilin (2) (14 mg, 0.025 mmole), *S*-(+)-alanine methyl ester hydrochloride (35 mg, 0.25 mmole), diphenylphosphoryl azide (28 mg, 0.25 mmole) and triethyl amine (51 mg, 0.5 mmole) were mixed in 0.5 mL of dry dimethyl sulfoxide at room temperature. The reaction was carried out as above, and in an identical work-up gave 8.2 mg of bis-amide (4) (45% yield). It had mp 139-141°C; $[\alpha]_{589}^{25}$ = +330° (*c* 0.02, $CH_2Cl_2$); IR (deposition from $CH_2Cl_2$) $\nu$: 3435, 2934, 1750, 1675, 1680, 1645 $cm^{-1}$; $^1$H-NMR ($CDCl_3$) $\delta$: 1.25 (d, 6H, J=7 Hz), 1.87 (s, 3H), 1.99 (s, 3H), 2.14 (s, 3H), 2.48 (t, 4H), 2.91 (t, 4H), 3.74 (s, 3H), 4.64 (q, 2H), 5.96 (s, 2H), 10.25 (d, 2CONH-, J=7 Hz), 10.62 (s, 2NH), 11.70 (s, 2NH) ppm.

*Anal.* Calcd. for $C_{39}H_{50}N_6O_8$ (730): C, 64.09; H, 6.90; N, 11.50
Found: C, 64.28; H, 6.98; N, 11.28

**Molecular Dynamics.** Molecular mechanics calculations and molecular modelling were carried out on an Evans and Sutherland ESV-10 workstation using version 5.41 of SYBYL (Tripos Assoc., St. Louis, MO). The dipyrrinone units of **1** and **2** were rotated independently about the central $C(CH_3)_2$ or $-CH_2-$ at C(10) (torsion angles $\phi_1$ and $\phi_2$) through 10° increments from 0° to 360°. (The $\phi_1=0°$, $\phi_2=0°$ conformer has a porphyrin shape.) In this procedure, the two torsion angles were held fixed at each increment while the remainder of the molecule was relaxed to its minimum energy conformation using molecular mechanics. This was followed by a molecular dynamics cooling curve consisting of the following temperatures and times: 100 fs at 20°K, 100 fs at 10°K, 100 fs at 5°K, 200 fs at 2°K, 200 fs at 1°K, 200 fs at 0.5°K, 300 fs at 0.1°K. This was followed by molecular mechanics minimization, which gave the lowest energy conformations for each set of $\phi$ values. The conformational energy maps were created using Wingz™ (Informix), and the ball and stick drawings were created from the atomic coordinates of the molecular dynamics structures using Müller and Falk's "Ball and Stick" program (Cherwell Scientific, Oxford, U.K.) for the Macintosh.

**Acknowledgements** We thank the National Institutes of Health (HD17779) for generous support.

## REFERENCES AND NOTES

1. For leading references see Lightner, D.A.; McDonagh, A.F. *Acc. Chem. Res.* **1984**, *17*, 417-424.
2. Ostrow, J.D., ed. *Bile Pigments and Jaundice*; Marcel Dekker: New York, 1986.
3. For leading references see Falk, H. *The Chemistry of Linear Oligopyrroles and Bile Pigments*, Springer Verlag, New York, 1989.
4. Lightner, D.A.; Person, R.V.; Peterson, B.R.; Puzicha, G.; Pu, Y-M.; Bojadziev, S. *Biomolecular Spectroscopy II* (Birge, R.R.; Nafie, L.A., eds.), Proc. SPIE *1432*, **1991**, 2-13.
5. (a) Bonnett, R.; Davies, J. E.; Hursthouse, M. B.; Sheldrick, G. M. *Proc. R. Soc. London, Ser. B* **1978**, *202*, 249-268.
   (b) LeBas, G.; Allegret, A.; Mauguen, Y.; DeRango, C.; Bailly, M. *Acta Crystallogr., Sect. B* **1980**, *B36*, 3007-3011.
   (c) Becker, W.; Sheldrick, W.S. *Acta Crystallogr., Sect. B* **1978**, *B34*, 1298-1304.
   (d) Mugnoli, A.; Manitto, P.; Monti, D. *Acta Crystallogr.* **1983**, *C38*, 1287-1291.
   (e) Becker, W.; Sheldrick, W.S. *Acta Crystallogr., Sect. B34* **1978**, 1298-1304.
6. (a) Kaplan, D.; Navon, G. *Isr. J. Chem.* **1983**, *23*, 177-186.
   (b) Kaplan, D.; Navon, G. *Org. Magn. Res.*, 198.
   (c) Kaplan, D.; Navon, G. *Biochem. J.* **1982**, *201*, 605-613.
   (d) Navon, G.; Frank, S.; Kaplan, D. *J. Chem. Soc. Perkin Trans. 2* **1984**, 1145-1149.
   (e) Manitto, P.; Monti, D. *J. C. S. Chem. Commun.* **1976**, 122-123.
7. Barnes, J.C.; Paton, J.D.; Damewood, J.R. Jr., Mislow, K. *J. Org. Chem.* **1981**, *46*, 4975-4979.
8. Xie, M.; Lightner, D.A. *Tetrahedron* **1993**, *49*, in press.
9. Trull, F.R.; Franklin, R.W.; Lightner, D.A. *J. Heterocyclic Chem.* **1987**, *24*, 1573-1579.
10. (a) Falk, H., Müller, N. *Monatsh. Chem.* **1982**, *112*, 1325-1332.
    (b) Falk, H., Müller, N. *Tetrahedron* **1983**, *39*, 1875-1885.
11. Along the interconversion pathway connecting *P* and *M* chirality global minimum enantiomers, carbon-carbon bond rotations in the propionic acid segments bring the rear-facing $\beta$-$CH_2$ groups of *P* [(60°, 60°) Fig. 6] into a forward position and turn the front-facing $\alpha$-$CH_2$ groups to the rear. These positional inversions appear to take place most easily near the local minimum [(120°, 120°) Fig. 6]. The conformation at (120°, 120°) without such rotations is higher energy (~2 kcal/mole).
12. Trull, F.R.; Ma, J.S.; Landen, G.L.; Lightner, D.A. *Israel J. Chem.* **1983**, *23 (2)*, 211-218.
13. See for example, Lightner, D.A.; Bouman, T.D.; Crist, B.V.; Rodgers, S.L.; Knobeloch, M.A.; Jones, A.M. *J. Am. Chem. Soc.* **1987**, *109*, 6248-6259.
14. Lightner, D.A.; Gawroński, J.K.; Wijekoon, W.M.D. *J. Am. Chem. Soc.* **1987**, *109*, 6354-6362.
15. Gawroński, J.K.; Połonski, T.; Lightner, D.A. *Tetrahedron* **1990**, *46*, 8053-8066.
16. Lightner, D.A.; Wijekoon, W.M.D.; Zhang, M-H. *J. Biol. Chem.* **1988**, *263*, 16669-16676.
17. Puzicha, G.; Pu, Y-M.; Lightner, D.A. *J. Am. Chem. Soc.* **1991**, *113*, 3583-3592.